Enhanced killing of SCC17B human head and neck squamous cell carcinoma cells after photodynamic therapy plus fenretinide via the *de novo* sphingolipid biosynthesis pathway and apoptosis

NITHIN B. BOPPANA[1], URSULA STOCHAJ[3], MOHAMED KODIHA[3], ALICJA BIELAWSKA[4],
JACEK BIELAWSKI[4], JASON S. PIERCE[4], MLADEN KORBELIK[5] and DUSKA SEPAROVIC[1,2]

[1]Department of Pharmaceutical Sciences, Eugene Applebaum College of Pharmacy and Health Sciences, and
[2]Karmanos Cancer Institute, Wayne State University, Detroit, MI 48201, USA; [3]Department of Physiology,
McGill University, Montreal, QC H3G 1YC, Canada; [4]Department of Biochemistry and
Molecular Biology, Medical University of South Carolina, Charleston, SC 29425, USA;
[5]British Columbia Cancer Agency, Vancouver, BC V5Z 1L3, Canada

Abstract. Because photodynamic therapy (PDT) alone is not always effective as an anticancer treatment, PDT is combined with other anticancer agents for improved efficacy. The clinically-relevant fenretinide [N-(4-hydroxyphenyl) retinamide; 4HPR], was combined with the silicon phthalocyanine photosensitizer Pc4-mediated PDT to test for their potential to enhance killing of SCC17B cells, a clinically-relevant model of human head and neck squamous cell carcinoma. Because each of these treatments induces apoptosis and regulates the *de novo* sphingolipid (SL) biosynthesis pathway, the role of ceramide synthase, the pathway-associated enzyme, in PDT+4HPR-induced apoptotic cell death was determined using the ceramide synthase inhibitor fumonisin B1 (FB). PDT+4HPR enhanced loss of clonogenicity. zVAD-fmk, a pan-caspase inhibitor, and FB, protected cells from death post-PDT+4HPR. In contrast, the anti-apoptotic protein Bcl2 inhibitor ABT199 enhanced cell killing after PDT+4HPR. Combining PDT with 4HPR led to FB-sensitive, enhanced Bax associated with mito-chondria and cytochrome *c* redistribution. Mass spectrometry data showed that the accumulation of C16-dihydroceramide, a precursor of ceramide in the *de novo* SL biosynthesis pathway, was enhanced after PDT+4HPR. Using quantitative confocal microscopy, we found that PDT+4HPR enhanced dihydrocer-amide/ceramide accumulation in the ER, which was inhibited by FB. The results suggest that SCC17B cells are sensitized to PDT by 4HPR via the *de novo* SL biosynthesis pathway and apoptosis, and imply potential clinical relevance of the combination for cancer treatment.

Introduction

Photodynamic therapy (PDT), a clinically-approved cancer therapy, utilizes a photosensitizer, a light at a wavelength corresponding to the photosensitizer's absorbance, and molec-ular oxygen to produce reactive oxygen species in malignant cellular targets, and ultimately causing their destruction (1). Apoptosis is an important mechanism for eliminating tumors (2-6), and the effectiveness of PDT regimens correlates with tumor cell apoptosis (7). Because PDT itself is not always effective as a tumor treatment (8,9), PDT is combined with other anticancer agents for improved therapeutic benefit. 4HPR [N-(4-hydroxyphenyl) retinamide; fenretinide], a proapoptotic, clinically-relevant anticancer synthetic retinoid (10), is a potential candidate for combined treatment.

As others and we have shown, sphingolipids (SLs), e.g., ceramide, generated via the *de novo* SL biosynthetic pathway (Fig. 1), have been implicated in apoptotic cell death after PDT and 4HPR in various malignant cell lines (11-14). Ceramide synthase catalyzes a reaction in the *de novo* SL biosynthesis pathway, in which a fatty acyl group is added to dihydro-sphingosine to form dihydroceramide. Ceramide is formed in the subsequent desaturase-dependent reaction, which can be inhibited by 4HPR (15). The ceramide synthase inhibitor fumonisin B1 (FB) renders cells resistant to apoptosis after PDT and 4HPR (14,16).

There have been no reports on combining PDT with 4HPR for improving the efficacy of PDT. The objective of the present study was to test the hypothesis that combining PDT with 4HPR enhances cell killing via apoptosis and the *de novo* SL biosynthesis pathway. We used SCC17B cells, a human head and neck squamous cell carcinoma cell line, representing a model that is potentially PDT-treatable in the clinic (17).

Correspondence to: Dr Duska Separovic, Department of Pharma-ceutical Sciences, Eugene Applebaum College of Pharmacy and Health Sciences, Wayne State University, 259 Mack Ave, Detroit, MI 48201, USA
E-mail: dseparovic@wayne.edu

Materials and methods

Materials. The phthalocyanine photosensitizer Pc4, $HOSiPcOSi(CH_3)_2(CH_2)_3N(CH_3)_2$, was kindly provided by Dr Malcolm E. Kenney (Department of Chemistry, Case Western Reserve University, Cleveland, OH, USA). 4HPR [N-(4-hydroxyphenyl) retinamide], fetal bovine serum and goat serum were purchased from Sigma-Aldrich (St. Louis, MO, USA). Cellgro DMEM/F-12 medium was obtained from Thermo Fisher Scientific (Waltham, MA, USA). Inhibitors were from the sources indicated in brackets: zVAD-fmk (MBL International Corp., Woburn, MA, USA), fumonisin B1 (Cayman Chemicals, Ann Arbor, MI, USA) and ABT-199 (Selleck Chemicals, Houston, TX, USA).

Cell culture and treatments. SCC17B cells were obtained from Dr Thomas Carey (University of Michigan, Ann Arbor, MI, USA). Cells were grown in DMEM/F-12 medium containing 10% fetal bovine serum, 100 U/ml penicillin and 100 μg/ml streptomycin (Life Technologies, Carlsbad, CA, USA) in a humidified incubator at 37˚C and 5% CO_2. For all experiments, unless indicated otherwise, incubation of cells was carried out in a humidified incubator at 37˚C and 5% CO_2. All treatments, as well as staining with Mitotracker Red CMXRos (see below) were added to cells in growth medium. After overnight incubation with Pc4 (20 nM), 4HPR (2.5 μM) was added immediately prior to irradiation. Cells were irradiated at room temperature with red light (2 mW/cm^2; λ_{max} ~670 nm) using a light-emitting diode array light source (EFOS, Mississauga, ON, Canada) at the fluence of 200 mJ/cm^2 and incubated for 10 h. Phosphate-buffered saline (PBS) without calcium and magnesium was used for confocal microscopy. PBS containing calcium and magnesium was used for mass spectrometry (MS). Both types of PBS were purchased from Life Technologies.

Clonogenic assay. Cell survival was assessed using clonogenic assay according to the modified pre-plating protocol, as we have described (18). Cells were resuspended in growth medium containing Pc4 (20 nM) and seeded (250 cells/well) in a 6-well plate (Thermo Fisher Scientific). After overnight incubation, the cells were irradiated. 4HPR was added immediately prior to irradiation. The inhibitors FB, zVAD-fmk (zVAD) and ABT-199 (ABT) were added 1 h prior to PDT±4HPR. After 14 days of incubation, the medium was aspirated, the plates were stained with crystal violet (0.1% in 20% ethanol; Sigma-Aldrich) for 30 sec, rinsed with water and air-dried. Colonies (≥50 cells) were counted using eCount Colony Counter (VWR International, Radnor, PA, USA). Plating efficiency was 36% (n=16).

Quantitative confocal microscopy. Cells were grown on coverslips (Thermo Fisher Scientific) in 6-well plates (Thermo Fisher Scientific). To visualize mitochondria, treated cells were incubated with Mitotracker Red CMXRos (250 nM; Life Technologies) in growth medium for 30 min. After treatments, the coverslips were washed with cold PBS, and fixed by incubation for 15 min in 4% formaldehyde (Thermo Fisher Scientific) in PBS. After washing with PBS, cells were permeabilized with ice-cold acetone/methanol (1:1) for 10 min. After blocking with
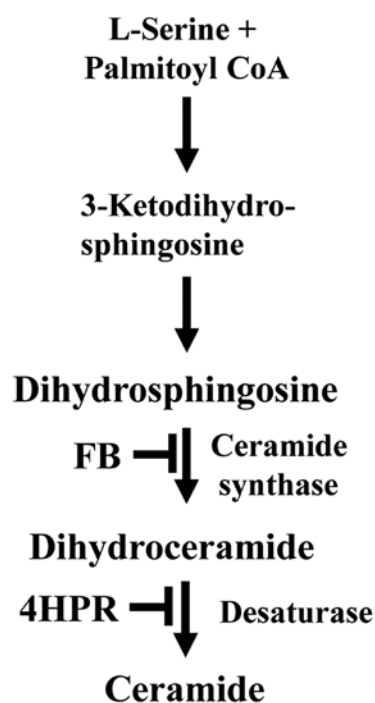

Figure 1. *De novo* SL biosynthesis pathway is FB- and 4HPR-sensitive.

3% goat serum and 3% fetal bovine serum in PBS for 1 h at 4˚C, cells were incubated at room temperature for 45 min with mouse monoclonal anti-dihydroceramide/ceramide antibodies (1:30; ALX-804-196; Enzo Life Sciences, Ann Arbor, MI, USA). After washing with cold PBS, cells were incubated at room temperature for 45 min with Alexa 488-conjugated goat anti-mouse monoclonal IgM antibodies (1:200; 115-546-075; Jackson ImmunoResearch, West Grove, PA, USA) and washed again with cold PBS. To visualize the nuclei, cells were stained with 4'6-diamidino-2-phenylindole (DAPI; Life Technologies; 1 μg/ml in cold PBS) for 10 min at room temperature and washed with cold PBS. The coverslips were mounted on slides using the ProLong Antifade kit (P7481; Life Technologies). Zeiss LSM780 confocal microscope equipped with a 100x1.4 NA OIL DIC D objective (Carl Zeiss, Thornwood, NY, USA) was used for acquiring the images.

For ER and dihydroceramide/ceramide detection, mouse monoclonal anti-KDEL antibody (1:50; ab12223; Abcam, Cambridge, MA, USA) and anti-dihydroceramide/ceramide antibodies were combined with Alexa 594-conjugated goat anti-mouse IgG (115-585-071) and Alexa 488-conjugated goat anti-mouse IgM antibodies (both 1:200; monoclonal, from Jackson ImmunoResearch), respectively. For visualization of Bax, mouse monoclonal anti-Bax antibodies (1:50; ab5714; Abcam) were combined with Alexa 488-conjugated monoclonal goat anti-mouse IgG antibodies (1:200; 115-545-071; Jackson ImmunoResearch). For visualization of cytochrome *c* (cyt *c*) redistribution, mouse monoclonal anti-cyt *c* antibodies (1:50; 556432; BD Biosciences, San Jose, CA, USA) were combined with Alexa 594-conjugated goat anti-mouse IgG (1:200; Jackson ImmunoResearch). As a criterion to score the cells positive for the redistribution of cyt *c* the margin of cyt *c* staining around the nuclei greater than 10 μm was used. At least 100 cells were assessed for every condition in each experiment. Confocal

microscopy imaging was performed at the Microscopy, Imaging and Cytometry Resources Core at Wayne State University, School of Medicine.

Quantifications were carried out as follows: dihydroceramide/ceramide fluorescence associated with the ER and the mitochondria, as well as Bax fluorescence associated with the mitochondria, were all quantified with MetaXpress software (version 5 5.00.20; Molecular Devices, LLC; Sunnyvale, CA, USA) (19). Mitotracker or anti-KDEL antibodies were employed to demarcate the mitochondria or the ER. Dihydroceramide/ceramide or Bax-pixel intensities associated with these subcellular compartments were measured with the multiwavelength cell scoring module. The correct compartment identification was verified by visual inspection. All images were corrected for background contribution before quantification. For Bax associated with mitochondria a minimum of 488 regions were measured for each data point. For dihydroceramide/ceramide associated with the ER and mitochondria a minimum of 680 or 518 regions were measured for each data point, respectively. Significant differences (p<0.05) were determined using comparison of multiple samples by one-way ANOVA.

Electrospray ionization/double mass spectrometry (MS) analysis. After treatments, cells were collected on ice, washed twice with cold PBS, resuspended in a mixture of ethyl acetate/methanol (1:1, v/v; EMD Millipore, Billerica, MA, USA), dried under nitrogen in the N-EVAP analytical evaporator (Organomation; Berlin, MA, USA), and shipped overnight on dry ice to the Lipidomics Shared Resource Facility (Medical University of South Carolina, Charleston, SC, USA) for further processing. After extraction, SLs were separated by high performance liquid chromatography, introduced to the electrospray ionization source and then analyzed by double MS using TSQ 7000 triple quadrupole mass spectrometer (Thermo-Fisher Scientific) as described previously (20). The pmoles of SLs were normalized per mg protein. Protein content was determined by a modified Bradford assay per manufacturer's instructions (Bio-Rad, Hercules, CA, USA).

Statistical analysis. Significant differences (p<0.05) were determined using Student's t-test or one-way ANOVA.

Results

Enhanced cell killing after PDT+4HPR is FB-, zVAD-fmk- and ABT-199-sensitive. Clonogenic assay was used to test whether combining PDT with 4HPR sensitizes SCC17B cells to PDT. As shown in Table I, when PDT and 4HPR were used at LD20 each, i.e., the dose reducing survival by 20%, 63% of PDT+4HPR-treated cells were unable to form colonies. To determine whether apoptosis and ceramide synthase are necessary for enhanced cell killing after PDT+4HPR, we used the pancaspase inhibitor zVAD-fmk (zVAD), the Bcl2 inhibitor ABT-199 (ABT), and the ceramide synthase inhibitor FB (21-23). We have previously shown that FB and zVAD rendered cells resistant to PDT (16). In contrast, ABT sensitized cells to PDT (16). Apoptosis is a major pathway involved in the anti-cancer action of 4HPR (24) and the *de novo* SL biosynthesis pathway plays a role in 4HPR-induced apoptosis (14,25). As

Table I. PDT+4HPR-induced augmented cell killing is FB-, zVAD- and ABT-sensitive in SCC17B cells.

Treatment	% Survival
FB	96±0.9
zVAD	96±0.8
ABT	97±1.3
4HPR	80±0.6[a]
4HPR+FB	91±0.9[a,b]
4HPR+zVAD	95±1.0[b]
4HPR+ABT	73±0.7[a,b]
PDT	79±0.6[a]
PDT+FB	93±0.7[b]
PDT+zVAD	91±1.3[a,b]
PDT+ABT	67±2.2[a,b]
PDT+4HPR	37±0.7[a,c]
PDT+4HPR+FB	73±1.7[a,b]
PDT+4HPR+zVAD	91±1.6[b]
PDT+4HPR+ABT	32±0.9[a,b]

FB, zVAD (10 μM each) and ABT (0.1 μM) were added 1 h prior to PDT (20 nM Pc4+200 mJ/cm^2), 4HPR (2.5 μM) or the combination. Colonies were stained with crystal violet (0.1%) and counted 14 days after treatments. The data are shown as the average ± SEM (n=3-18 samples). Significant differences are shown between: [a]treatment and untreated control; [b](treatment + inhibitor) and treatment; [c]combination and individual treatments.

shown in Table I, all inhibitors were non-toxic (LD<5). FB and zVAD rendered the cells resistant not only to PDT and 4HPR alone, but also to PDT+4HPR. In contrast, ABT sensitized SCC17B cells to PDT±4HPR.

PDT+4HPR-enhanced Bax associated with mitochondria and cyt c redistribution is inhibited by FB. The mitochondrial apoptosis pathway, including Bax translocation to mitochondria and cyt *c* redistribution/release, is induced by PDT and 4HPR (16,26-28). Both of these processes are inhibited by FB after PDT (16). The question is whether the mitochondrial apoptosis pathway is affected by combining PDT with 4HPR, and whether the process is ceramide synthase-dependent. Using quantitative confocal microscopy we found that Bax associated with mitochondria and cyt *c* redistribution were induced after each individual treatment (Fig. 2). PDT+4HPR enhanced Bax associated with mitochondria and cyt *c* redistribution, and FB inhibited both processes.

PDT+4HPR enhances C16-dihydroceramide, not ceramide, accumulation. Both PDT and 4HPR regulate the *de novo* SL biosynthesis pathway (12-16,29). The question is what the effects of combining PDT with 4HPR on the cellular SL profile are. We used MS to address the question. As depicted in Fig. 3A, in contrast to 4HPR, PDT increased total ceramide
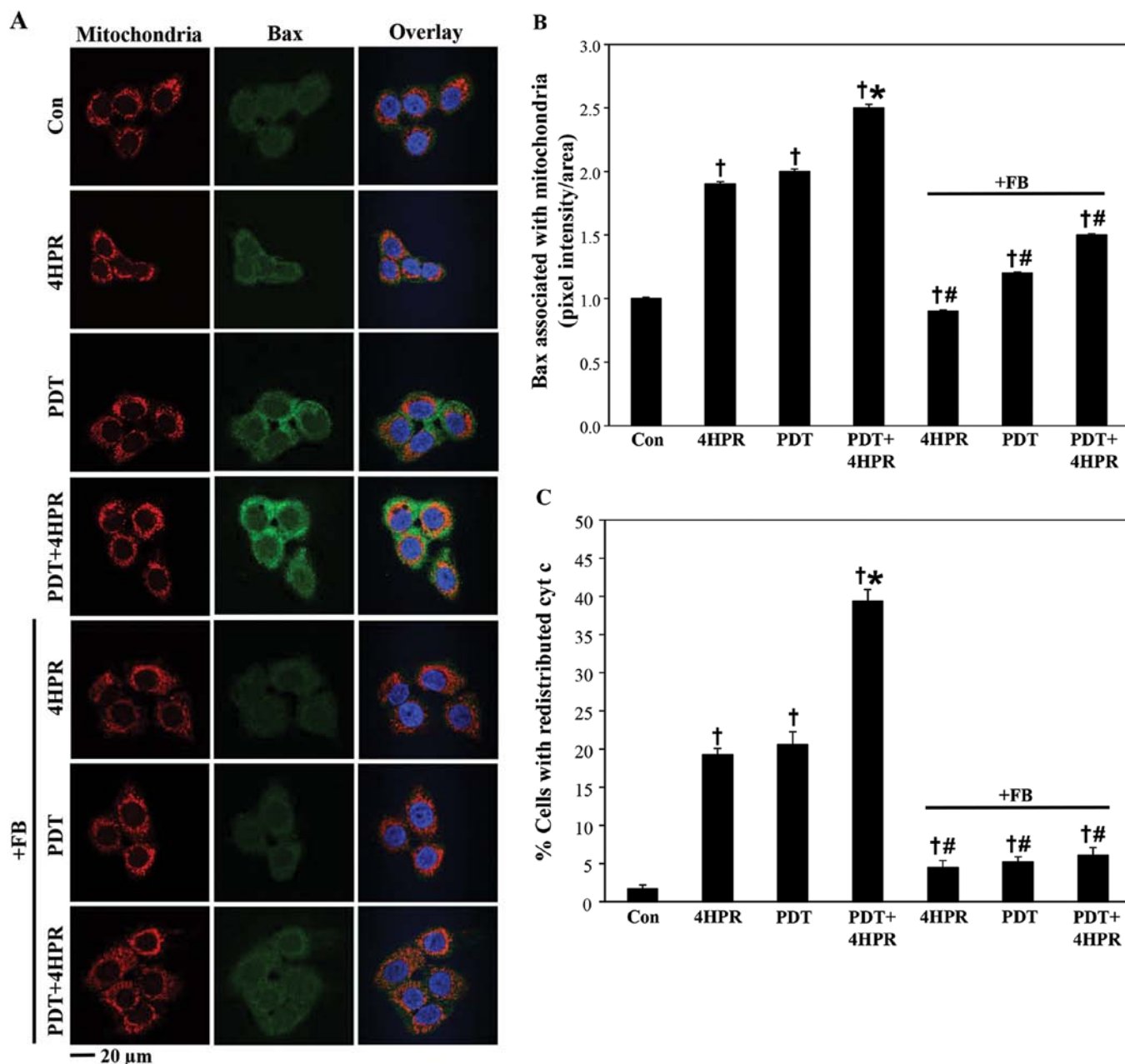
Figure 2. PDT+4HPR-induced enhanced Bax associated with mitochondria and cyt *c* redistribution are inhibited by FB. FB (10 μM) was added 1 h prior to PDT (20 nM Pc4 + 200 mJ/cm^2; LD20), 4HPR (2.5 μM; LD20) or the combination. Incubation time was 10 h post-treatments. After treatments, cells were immunostained with anti-Bax antibodies (A and B) or anti-cyt *c* antibodies (C). Incubation with Mitotracker Red CMXRos was carried out prior to immuno-staining with anti-Bax antibodies (A and B). Nuclei were visualized with DAPI. Images were acquired by confocal microscopy using identical settings. (B) Bax fluorescence located in the mitochondria was quantified with MetaXpress software. The graph shows Bax fluorescence/mitochondrial area. The data were normalized to the untreated control. Results are shown as the average ± SEM. (C) To calculate percentages of cells with redistributed cyt *c*, at least 100 cells were scored for every sample. Each bar indicates an average ± SEM from 3-4 samples. (B and C) Significant differences are shown between: [†]treatment and untreated control; [#](treatment + inhibitor) and treatment; [*]combination and individual treatments. Con, untreated control.

accumulation. Combining PDT with 4HPR attenuated PDT-induced increase in total ceramide levels. The accumulation of individual ceramides, by and large, followed the same pattern (Table II). 4HPR did not significantly raise the levels of any individual ceramide. In contrast, 4HPR increased accumulation of C16-dihydroceramide, a *de novo* SL biosynthesis pathway metabolite by 445% above basal levels (Fig. 3B). PDT also increased the levels of C16-dihydroceramide by 138% beyond resting levels. Combining PDT with 4HPR enhanced accumulation of C16-dihydroceramide by 632%.

PDT+4HPR-induced enhanced ceramide accumulation in the ER is inhibited by FB. Because the *de novo* SL biosynthesis pathway is localized to the ER, we tested the effect of combining PDT with 4HPR on dihydroceramide/ceramide accumulation in the ER. Using an antibody that recognizes dihydroceramide and ceramide (30) and the ER marker anti-KDEL for quantitative confocal microscopy, we found that PDT+4HPR enhanced dihydroceramide/ceramide accumulation in the ER (Fig. 4A and B). FB inhibited ER-associated ceramide accumulation after PDT±4HPR.
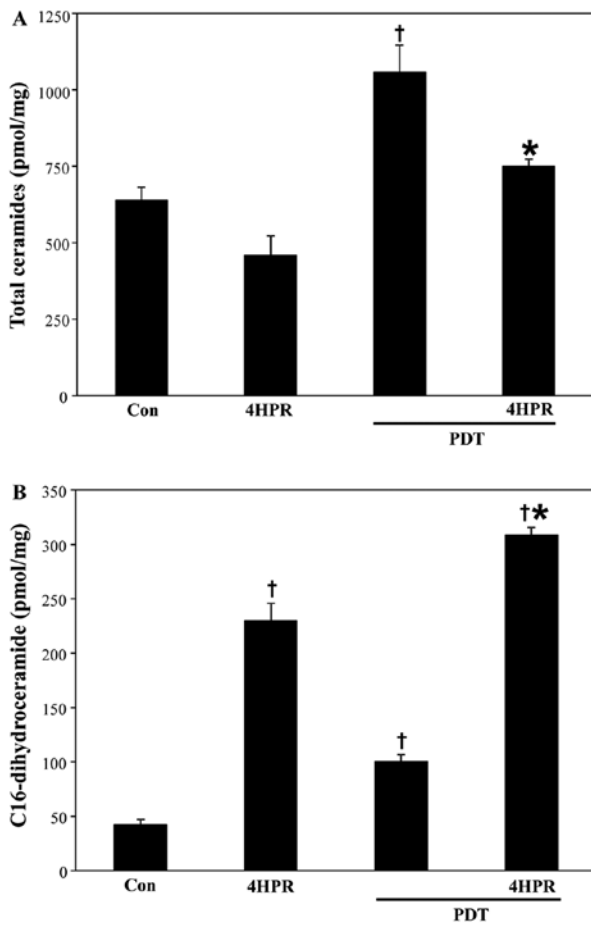
Figure 3. (A) Effect of PDT±4HPR on total ceramide levels. (B) PDT+4HPR enhances C16-dihydroceramide accumulation. Cells were treated with PDT (20 nM Pc4 + 200 mJ/cm^2; LD20), 4HPR (2.5 μM; LD20) or the combination, incubated for 10 h, collected and processed for MS. The levels of SLs were calculated as pmoles/mg protein and are shown as the average ± SEM (n=3-4). Significant differences are shown between: [†]treatment and untreated control; [*]combination and individual treatments. Con, untreated control. PDT alone data from ref. 16.

We have shown that PDT-induced mitochondrial dihydroceramide/ceramide accumulation is FB-sensitive (16). However, it is unknown what impact on mitochondrial dihydroceramide/ceramide accumulation combining PDT with 4HPR might have. Using the same anti-dihydroceramide/ceramide antibody and the mitochondrial marker Mitotracker for quantitative confocal microscopy, we found that PDT and 4HPR alone did induce mitochondrial dihydroceramide/ceramide accumulation (Fig. 4C). However, the effect was not enhanced after PDT+4HPR. FB inhibited mitochondrial ceramide accumulation after all the treatments.

Discussion

The present study is novel because, to our knowledge, no report exists on combining PDT with 4HPR. The results suggest that PDT+4HPR-induced enhanced killing of SCC17B cells depends on ceramide synthase, caspase activation and inhibition of Bcl2, and is associated with ceramide synthase-dependent mitochondrial apoptosis pathway. We have reported similar findings after PDT alone (16). In contrast, in breast cancer cells FB did not affect cell death after 4HPR (14). The discrepancy between the findings could be due to the use of different assays, i.e. clonogenic vs. short-term viability assay, respectively (31), or cell type-specificity of FB-induced resistance.

Our observation that 4HPR increased the levels of C16-dihydroceramide, the substrate of desaturase in the *de novo* SL biosynthesis pathway (Fig. 1), is consistent with the report showing 4HPR-induced inhibition of the enzyme (15). Our present findings that PDT-induced increased ceramides and C16-dihydroceramide in cells undergoing apoptosis are similar to our previous results in SCCVII mouse squamous carcinoma cells (18,32). Here we also demonstrate that combining PDT with 4HPR enhances C16-dihydroceramide levels, apoptosis and loss of clonogenicity. In addition, total ceramide levels, as well as most of the individual ceramides

Table II. Effect of PDT±4HPR on individual ceramides in SCC17B cells.

Ceramide	Con	4HPR	PDT	PDT+4HPR
C14-ceramide	16.1±0.9	16.7±1.8	29.4±1.7[a]	22.6±0.8[a,d]
C16-ceramide	91.0±11.9	51.7±6.4[a]	129.6±8.5[a]	93.5±3.6[d]
C18-ceramide	17.8±2.1	21.5±3.0	61.6±4.2[a]	48.3±0.8[a,d]
C18:1-ceramide	7.6±0.3	10.8±1.1	25.5±2.6[a]	22.4±0.8[a,b]
C20-ceramide	5.2±0.7	9.1±0.5	21.4±1.8[a]	17.6±1.2[a,b]
C20:1-ceramide	1.5±0.2	2.3±0.2	5.3±0.6[a]	3.9±0.3[a]
C22-ceramide	51.6±2.7	37.5±3.2	132.7±10.6[a]	100.3±3.0[a,d]
C22:1-ceramide	18.7±1.7	16.1±1.9	49.6±4.5[a]	34.6±1.5[a,d]
C24-ceramide	161.9±9.1	97.7±5.1	252.6±22.4[a]	175.2±8.9[d]
C24:1-ceramide	199.3±9.4	110.0±8.6[a]	305.4±28.6[a]	196.7±9.0[d]
C26-ceramide	15.8±3.6	10.6±0.8	13.9±1.3	11.0±1.0
C26:1-ceramide	33.4±3.2	20.1±1.8[a]	33.5±2.3	23.0±2.3[a,c]

SCC17B cells were treated with PDT (20 nM Pc4+200 mJ/cm^2), 4HPR (2.5 μM) or the combination, incubated for 10 h, collected, and processed for MS. Ceramide levels were calculated as pmoles/mg protein and are shown as the average ± SEM (n=3-4). Significant differences are shown between: [a]treatment and untreated control; [b]combination and 4HPR; [c]combination and PDT; [d]combination and both individual treatments. Con, untreated control. PDT alone data from ref. 16.
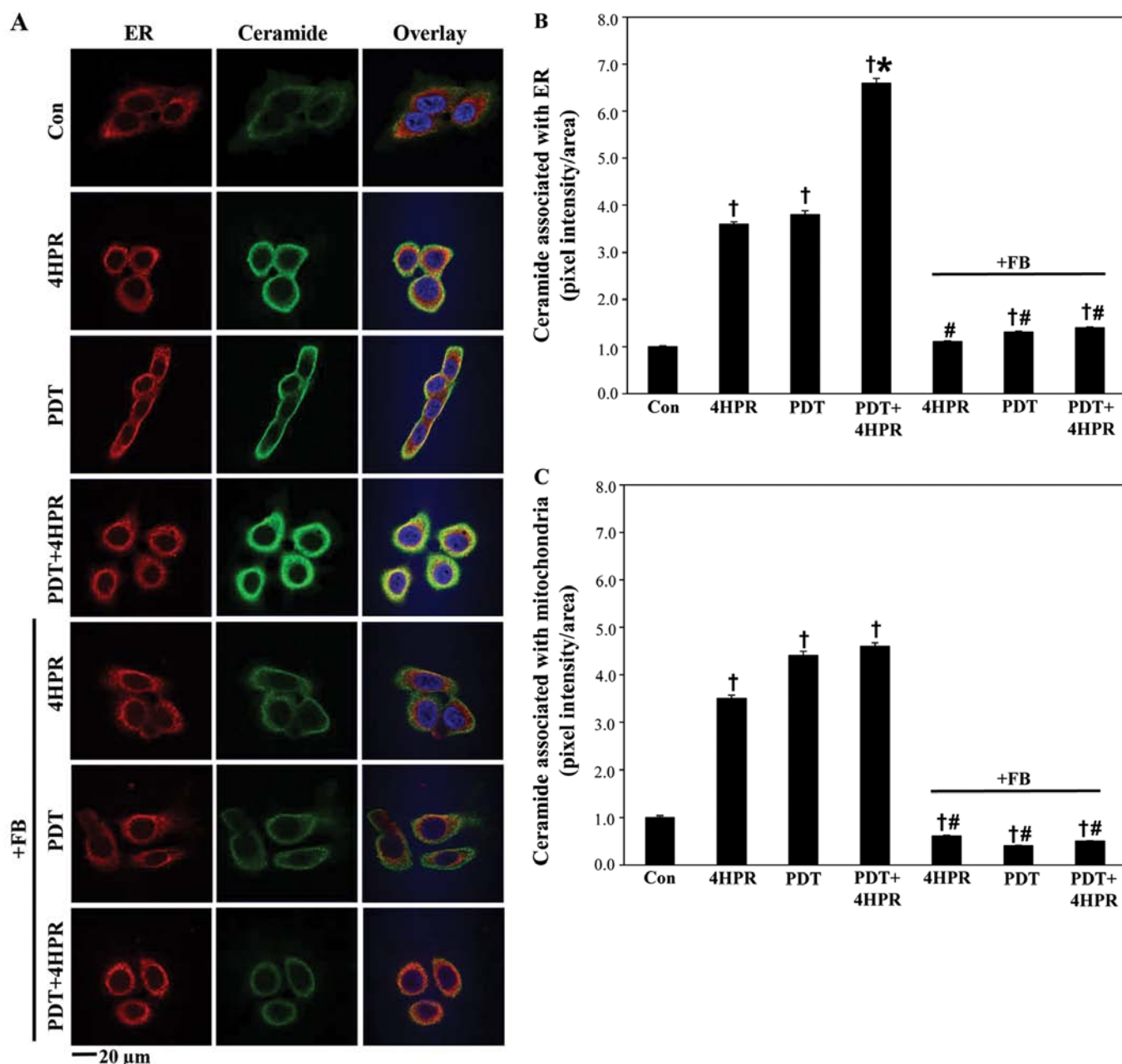
Figure 4. (A and B) PDT+4HPR-enhanced ceramide accumulation in the ER is inhibited by FB. (C) FB inhibits ceramide accumulation in mitochondria after PDT±4HPR. Cells were treated with FB (10 μM) 1 h prior to PDT (20 nM Pc4 + 200 mJ/cm^2; LD20), 4HPR (2.5 μM; LD20), or the combination, incubated for 10 h, and immunostained with anti-ceramide and, with anti-KDEL antibodies (A, B). (C) Incubation with Mitotracker Red CMXRos was carried out prior to immunostaining with anti-ceramide antibodies. Nuclei were visualized with DAPI. All images were acquired by confocal microscopy with identical settings. MetaXpress software was used to quantify ceramide fluorescence located in the ER (B) and mitochondria (C). (B and C) Data are shown as the average ± SEM. The graphs depict ceramide fluorescence/ER area (B), or ceramide fluorescence/mitochondrial area (C). Results were normalized to the untreated control. Significant differences are shown between: [†]treatment and untreated control; [#](treatment + inhibitor) and treatment; [*]combination and individual treatments. Con, untreated control.

remained above baseline levels after PDT+4HPR. These data support the notion that dihydroceramide, together with ceramide, has a pro-apoptotic/pro-death role.

We demonstrate in the present report that PDT+4HPR-induced enhanced killing of SCC17B cells is associated with ER-localized and FB-sensitive *de novo* SL biosynthesis. This is in accordance with previous findings for PDT and 4HPR itself (15,16,29). Although each treatment alone increased mitochondrial dihydroceramide/ceramide accumulation in a FB-sensitive manner, combining PDT with 4HPR did not affect the process. The ER and mitochondria are connected by the mitochondria-associated membrane. Ceramide synthase activation has been shown in mitochondria-associated membrane after radiation (33). Reportedly, 4HPR can activate ceramide synthase (29). It remains to be established whether and at what subcellular site ceramide synthase is activated after PDT+4HPR.

We believe that our findings have important clinical implications. Combining PDT with another anticancer agent is advantageous because lower doses of individual treatments (LD20; Table I) are required for improved therapeutic benefit. This study also shows that combining PDT with 4HPR

enhances cell killing via the *de novo* SL biosynthesis and mitochondrial apoptotic pathway. Thus, targeting these pathways could augment the therapeutic value of PDT.

Acknowledgements

References

1. Agostinis P, Berg K, Cengel KA, Foster TH, Girotti AW, Gollnick SO, Hahn SM, Hamblin MR, Juzeniene A, Kessel D, Korbelik M, Moan J, Mroz P, Nowis D, Piette J, Wilson BC and Golab J: Photodynamic therapy of cancer: an update. CA Cancer J Clin 61: 250-281, 2011.
2. Boisteau O, Gautier F, Cordel S, Henry F, Harb J, Douillard JY, Vallette FM, Meflah K and Gregoire M: Apoptosis induced by sodium butyrate treatment increases immunogenicity of a rat colon tumor cell line. Apoptosis 2: 403-412, 1997.
3. Sato M, Harada K, Yura Y, Azuma M, Kawamata H, Iga H, Tsujimoto H, Yoshida H and Adachi M: The treatment with differentiation- and apoptosis-inducing agent, vesnarinone, of a patient with oral squamous cell carcinoma. Apoptosis 2: 313-318, 1997.
4. Schiffer IB, Gebhard S, Heimerdinger CK, Heling A, Hast J, Wollscheid U, Seliger B, Tanner B, Gilbert S, Beckers T, Baasner S, Brenner W, Spangenberg C, Prawitt D, Trost T, Schreiber WG, Zabel B, Thelen M, Lehr HA, Oesch F and Hengstler JG: Switching off HER-2/neu in a tetracycline-controlled mouse tumor model leads to apoptosis and tumor-size-dependent remission. Cancer Res 63: 7221-7231, 2003.
5. Stahnke K, Eckhoff S, Mohr A, Meyer LH and Debatin KM: Apoptosis induction in peripheral leukemia cells by remission induction treatment in vivo: selective depletion and apoptosis in a CD34+ subpopulation of leukemia cells. Leukemia 17: 2130-2139, 2003.
6. Urosevic M, Maier T, Benninghoff B, Slade H, Burg G and Dummer R: Mechanisms underlying imiquimod-induced regression of basal cell carcinoma in vivo. Arch Dermatol 139: 1325-1332, 2003.
7. Henderson BW, Gollnick SO, Snyder JW, Busch TM, Kousis PC, Cheney RT and Morgan J: Choice of oxygen-conserving treatment regimen determines the inflammatory response and outcome of photodynamic therapy of tumors. Cancer Res 64: 2120-2126, 2004.
8. Wilson JJ, Jones H, Burock M, Smith D, Fraker DL, Metz J, Glatstein E and Hahn SM: Patterns of recurrence in patients treated with photodynamic therapy for intraperitoneal carcinomatosis and sarcomatosis. Int J Oncol 24: 711-717, 2004.
9. Rhodes LE, de Rie M, Enstrom Y, Groves R, Morken T, Goulden V, Wong GA, Grob JJ, Varma S and Wolf P: Photodynamic therapy using topical methyl aminolevulinate vs surgery for nodular basal cell carcinoma: results of a multicenter randomized prospective trial. Arch Dermatol 140: 17-23, 2004.
10. Mariani L, Formelli F, De Palo G, Manzari A, Camerini T, Campa T, Di Mauro MG, Crippa A, Delle Grottaglie M, Del Vecchio M, Marubini E, Costa A and Veronesi U: Chemoprevention of breast cancer with fenretinide (4-HPR): study of long-term visual and ophthalmologic tolerability. Tumori 82: 444-449, 1996.
11. Dolgachev V, Nagy B, Taffe B, Hanada K and Separovic D: Reactive oxygen species generation is independent of de novo sphingolipids in apoptotic photosensitized cells. Exp Cell Res 288: 425-436, 2003.
12. Dolgachev V, Farooqui MS, Kulaeva OI, Tainsky MA, Nagy B, Hanada K and Separovic D: De novo ceramide accumulation due to inhibition of its conversion to complex sphingolipids in apoptotic photosensitized cells. J Biol Chem 279: 23238-23249, 2004.
13. Wispriyono B, Schmelz E, Pelayo H, Hanada K and Separovic D: A role for the de novo sphingolipids in apoptosis of photosensitized cells. Exp Cell Res 279: 153-165, 2002.
14. Rehman F, Shanmugasundaram P and Schrey MP: Fenretinide stimulates redox-sensitive ceramide production in breast cancer cells: potential role in drug-induced cytotoxicity. Br J Cancer 91: 1821-1828, 2004.
15. Kraveka JM, Li L, Szulc ZM, Bielawski J, Ogretmen B, Hannun YA, Obeid LM and Bielawska A: Involvement of dihydroceramide desaturase in cell cycle progression in human neuroblastoma cells. J Biol Chem 282: 16718-16728, 2007.
16. Boppana NB, Kodiha M, Stochaj U, Lin HS, Haimovitz-Friedman A, Bielawska A, Bielawski J, Divine GW, Boyd JA, Korbelik M and Separovic D: Ceramide synthase inhibitor fumonisin B1 inhibits apoptotic cell death in SCC17B human head and neck squamous carcinoma cells after pc4 photosensitization. Photochem Photobiol Sci 13: 1621-1627, 2014.
17. Biel MA: Photodynamic therapy of head and neck cancers. Methods Mol Biol 635: 281-293, 2010.
18. Separovic D, Saad ZH, Edwin EA, Bielawski J, Pierce JS, Van Buren E and Bielawska A: C16-ceramide analog combined with Pc 4 photodynamic therapy evokes enhanced total ceramide accumulation, promotion of DEVDase activation in the absence of apoptosis, and augmented overall cell killing. J Lipids 2011: 1-9, 2011.
19. Kodiha M, Brown CM and Stochaj U: Analysis of signaling events by combining high-throughput screening technology with computer-based image analysis. Sci Signal 1: l2, 2008.
20. Separovic D, Semaan L, Tarca AL, Awad Maitah MY, Hanada K, Bielawski J, Villani M and Luberto C: Suppression of sphingomyelin synthase 1 by small interference RNA is associated with enhanced ceramide production and apoptosis after photodamage. Exp Cell Res 314: 1860-1868, 2008.
21. Wang E, Norred WP, Bacon CW, Riley RT and Merrill AH Jr: Inhibition of sphingolipid biosynthesis by fumonisins. Implications for diseases associated with *Fusarium moniliforme*. J Biol Chem 266: 14486-14490, 1991.
22. Garcia-Calvo M, Peterson EP, Leiting B, Ruel R, Nicholson DW and Thornberry NA: Inhibition of human caspases by peptide-based and macromolecular inhibitors. J Biol Chem 273: 32608-32613, 1998.
23. Souers AJ, Leverson JD, Boghaert ER, Ackler SL, Catron ND, Chen J, Dayton BD, Ding H, Enschede SH, Fairbrother WJ, Huang DC, Hymowitz SG, Jin S, Khaw SL, Kovar PJ, Lam LT, Lee J, Maecker HL, Marsh KC, Mason KD, Mitten MJ, Nimmer PM, Oleksijew A, Park CH, Park CM, Phillips DC, Roberts AW, Sampath D, Seymour JF, Smith ML, Sullivan GM, Tahir SK, Tse C, Wendt MD, Xiao Y, Xue JC, Zhang H, Humerickhouse RA, Rosenberg SH and Elmore SW: ABT-199, a potent and selective BCL-2 inhibitor, achieves antitumor activity while sparing platelets. Nat Med 19: 202-208, 2013.
24. Hail N Jr, Kim HJ and Lotan R: Mechanisms of fenretinide-induced apoptosis. Apoptosis 11: 1677-1694, 2006.
25. Erdreich-Epstein A, Tran LB, Bowman NN, Wang H, Cabot MC, Durden DL, Vlckova J, Reynolds CP, Stins MF, Groshen S and Millard M: Ceramide signaling in fenretinide-induced endothelial cell apoptosis. J Biol Chem 277: 49531-49537, 2002.
26. Chiu SM, Xue LY, Usuda J, Azizuddin K and Oleinick NL: Bax is essential for mitochondrion-mediated apoptosis but not for cell death caused by photodynamic therapy. Br J Cancer 89: 1590-1597, 2003.
27. Tiwari M, Kumar A, Sinha RA, Shrivastava A, Balapure AK, Sharma R, Bajpai VK, Mitra K, Babu S and Godbole MM: Mechanism of 4-HPR-induced apoptosis in glioma cells: evidences suggesting role of mitochondrial-mediated pathway and endoplasmic reticulum stress. Carcinogenesis 27: 2047-2058, 2006.
28. Ulukaya E, Pirianov G, Kurt MA, Wood EJ and Mehmet H: Fenretinide induces cytochrome c release, caspase 9 activation and apoptosis in the absence of mitochondrial membrane depolarisation. Cell Death Differ 10: 856-859, 2003.
29. Wang H, Maurer BJ, Reynolds CP and Cabot MC: N-(4-hydroxyphenyl)retinamide elevates ceramide in neuroblastoma cell lines by coordinate activation of serine palmitoyltransferase and ceramide synthase. Cancer Res 61: 5102-5105, 2001.
30. Cowart LA, Szulc Z, Bielawska A and Hannun YA: Structural determinants of sphingolipid recognition by commercially available anti-ceramide antibodies. J Lipid Res 43: 2042-2048, 2002.

31. Oplustilova L, Wolanin K, Mistrik M, Korinkova G, Simkova D, Bouchal J, Lenobel R, Bartkova J, Lau A, O'Connor MJ, Lukas J and Bartek J: Evaluation of candidate biomarkers to predict cancer cell sensitivity or resistance to PARP-1 inhibitor treatment. Cell Cycle 11: 3837-3850, 2012.
32. Separovic D, Joseph N, Breen P, Bielawski J, Pierce JS, van Buren E, Bhatti G, Saad ZH, Bai A and Bielawska A: Combining anticancer agents photodynamic therapy and LCL85 leads to distinct changes in the sphingolipid profile, autophagy, caspase-3 activation in the absence of cell death, and long-term sensitization. Biochem Biophys Res Commun 409: 372-377, 2011.

33. Lee H, Rotolo JA, Mesicek J, Penate-Medina T, Rimner A, Liao WC, Yin X, Ragupathi G, Ehleiter D, Gulbins E, Zhai D, Reed JC, Haimovitz-Friedman A, Fuks Z and Kolesnick R: Mitochondrial ceramide-rich macrodomains functionalize Bax upon irradiation. PLoS One 6: e19783, 2011.